

Ten Years of Measurements of Tropical Upper-Tropospheric Water Vapor by MOZAIC: Climatology, Variability, Transport and Relation to Deep Convection

Zhengzhao Luo*, Dieter Kley[†] and Richard H. Johnson

Department of Atmospheric Science
Colorado State University
Fort Collins CO 80523

1. Introduction:

Atmospheric water vapor is the most important greenhouse gas in the climate system. It is highly variable on multiple spatial and temporal scales and has often been presumed to be increasing under a global warming scenario, resulting in an amplification of the CO₂ greenhouse effect (Cess et al. 1990). Unfortunately, water vapor in the troposphere is not measured with a high degree of accuracy, neither by the global radiosonde network nor by satellites. The difficulties are particularly compounded in the upper troposphere, where radiosonde humidity sensors fail at low temperature and satellite sensors provide only coarse vertical and horizontal resolution. Consequently, the distribution and source/sink processes of upper-tropospheric water vapor (UTWV) are at present not well understood.

In this study, effort is undertaken to fill an important gap in the knowledge of tropical upper-tropospheric humidity (UTH) temporal and spatial distributions and variability by employing high-quality water vapor measurements taken from MOZAIC (Measurement of Ozone and Water Vapor by Airbus In-Service Aircraft) for the period from 1994 to 2004. Three tropical regions are selected for detailed analysis due to their climatological importance and the geographical coverage of the MOZAIC flights: tropical Atlantic (30S-30N, 50W-10W), tropical Africa (30S-30N, 0E-40E), and Asian Monsoon region (EQ-30N, 60E-110E). In addition to a documentation of the climatology, we also compare the MOZAIC measurements with the ECMWF analysis highlighting the outstanding bias of the ECMWF. Finally, the relation of UTH distribution to large-scale transport and deep convection is explored by jointly studying the MOZAIC data and the ISCCP (International Satellite Cloud Climatology Project) data (Rossow et al. 1996; Rossow and Schiffer 1999), as well as the NCAR/NCEP reanalysis wind.

2. MOZAIC Data

MOZAIC is a project, funded by the European Union, for the measurement of the large-

*Corresponding author address: Dr. Zhengzhao Luo, Department of Atmospheric Science, Colorado State University, Fort Collins CO 80523
Email: luo@atmos.colostate.edu

[†] Also at Institut für Chemie und Dynamik der Geosphäre: Troposphäre Forschungszentrum Jülich, Jülich (Germany)

scale distribution of ozone and water vapor onboard commercial Airbus A340 aircraft during schedule flights (Marenco et al. 1998). Five A340 long-range passenger aircraft are equipped with semi-automated instrumentation to measure relative and specific humidity, ozone, temperature and to record aircraft data such as position, pressure, temperature, wind speed, Mach number etc. MOZAIC data on UTH (relative and specific) have a quality assured mean accuracy of 5% (Helten et al. 1998, 1999), which is superior to that of most other humidity data sources, including data from satellite instrumentation. UTH data with high vertical resolution, more accurate than those from MOZAIC, are only obtainable from campaign-style research instrumentation on dedicated balloons and research aircraft (Kley et al. 2000). The time resolution of the MOZAIC UTH measurements in the upper troposphere is 1 min which, at cruising speed, corresponds to a spatial resolution of 15 km. In the tropical regions, MOZAIC aircraft at cruise altitude fly at five discrete pressure levels of 288, 262, 238, 217 and 197 hPa¹. These altitudes are virtually always below the tropical tropopause layer (TTL). MOZAIC has been operational since August 1994. The flights cover all continents except Australia and all oceans except the Pacific (Fig. 1). Roughly 35% of flights cover the three tropical regions that are selected for a detailed study.

3. MOZAIC Climatology and Variability

Nawrath (2002) studied four years of MOZAIC climatology for the flights between Europe and South America covering the tropical Atlantic region. In this section, we expand her study by including more regions and covering a longer period of time. Moreover, we add the study of the composite annual cycle of UTH and its interannual/decadal variability.

3.1 UTH Annual Cycle

Figure 2 shows the composite annual cycle of UTH (with respect to ice) as a function of latitude for the three regions. In general, the seasonal migration of the UTH pattern keeps pace with that of the corresponding ITCZ at each region (Waliser and Gautier 1993), highlighting the convective influence

¹ The most common flight levels are 238 and 262 hPa for tropical Atlantic, 217 and 238 hPa for tropical Africa, and 217 and 288 hPa for the Asian Monsoon region.

on the UTH distribution. Some significant regional differences are identified: the magnitude of the UTH seasonal cycle is large for the South Asian Monsoon region and the tropical Africa; it is comparatively weak for the tropical Atlantic. The moistest upper troposphere is found in the Asian Monsoon region during the wet season, followed by the tropical Africa during the local summer, while it is least likely to see very moist upper troposphere in the tropical Atlantic. These regional differences are consistent with various previous works that show the differences in convective intensity among different tropical regions (e.g., Mohr and Zipser 1996) and will be discussed more in detail in Section 5.

3.2 UTH Vertical Structure

Figure 3 shows the height dependence of the UTH. Despite large standard deviation (due to the inclusion of different seasons), relative humidity generally increases with height. One explanation for this height dependence of UTH is that the upper levels correspond more closely to the convective detrainment layer, where there is an ejection of both saturated air and condensate serving as moisture source. Moreover, the lower levels may more often be subjected to subsidence drying. The prominent flight pressure levels vary with region and season; consequently, some levels have poorer coverage than others at certain locations during certain seasons. Nevertheless, the values at each pressure level in Fig. 3 are still based on hundreds to thousands of observations so that the statistical basis is strong. We performed a t-test for the tropical Atlantic to prove this: UTH at 197 hPa is statistically moister than that at 288 hPa at the confidence level higher than 99.9%.

3.3 UTH Distribution

Previous studies (e.g. Zhang et al. 2003) show that the instantaneous distribution of tropical UTH is bimodal. MOZAIC measurements corroborate this important result (Figs. 4 – 6). Moreover, they reveal some intriguing details pertaining to the bimodal distribution that were not previously identified. 1) In the deep tropics, the moisture level frequently reaches ice supersaturation and even approaches saturation over liquid. The most notable case is the Asian summer monsoon region where the UTH distribution almost becomes unimodal at ice saturation. The other extreme is the Southern Africa during the local winter, showing the driest upper troposphere among all regions with a dry mode at around 10%. Interestingly, the Sahara region is much wetter than Southern Africa having a mean UTH value that is twice as large. 2) The two modes in this bimodal distribution stay rather constant at around 20% and 100%; differences in the mean value are largely due to variations in the proportion of the two modes as opposed to changes in modes themselves. This suggests that the two dominant modes are probably a manifestation of two underlying processes that have controlling effects on UTH, presumably convective moistening and subsidence drying.

Horizontal large-scale transport also plays a role in affecting UTH (Sherwood 1996; Pierrehumbert and Roca 1998), but that the two UTH modes stay largely constant suggests the large-scale transport (which can be considered as having a homogenizing effect) probably operates on a longer time-scale such that the instantaneous distribution of UTH is dominated by the faster processes such as convection and subsidence (Mapes 2001; Zhang et al. 2003).

3.4 Interannual and Decadal Variability of UTH

Figure 7 shows the monthly mean UTH as a function of latitude and time. We apply a 4-month running average to the original data to smooth out some sporadic discontinuity in measurements. Large gaps, however, still exist, especially for the tropical Atlantic and the Asian Monsoon region from mid 2000 to early 2004. These gaps will affect a long-term study of the MOZAIC data over these regions. A noticeable interannual variability in Fig. 7 is associated with the ENSO event from late 1997 to mid 1998: the tropical Atlantic becomes drier during the El Niño phase (i.e., winter of 1997-1998) and the Asian Monsoon region gets moister during the following La Niña in the summer of 1998. Tropical Africa seems to be little affected by the ENSO event. Note that the magnitude of the interannual variability is generally weak for the three tropical regions because none of them lies near the maximum influence of the ENSO – the Pacific Ocean. Fig. 7 also shows an increase in UTH over the tropical Africa from year 2000 to 2002 (and maybe beyond). The reason for this increase is unknown. Since a minimum of three flights (with hundreds, if not thousands, of measurements) are required for each month to generate the monthly mean statistics (otherwise it will be labeled as having missing data) and this increase or upward trend is not short-lived but lasts for over two years, it is unlikely to be a sampling artifact. Moreover, there is no known problem with the measurement quality that can explain this change. More studies are needed to unravel the nature of this regional moistening trend.

4. Comparison to the ECMWF

The ECMWF analysis is produced operationally with a 4D-Var assimilation system. The analysis is performed at a horizontal resolution of T213 (roughly corresponding to 50 km); its vertical resolution increases from 31 levels to 60 levels over the course of the MOZAIC data period. To facilitate a comparison, the ECMWF analysis data are interpolated to the MOZAIC measurement coordinates on flights using a 3D cubic interpolation in space and a linear interpolation in time.

Figures 8 – 10 show the histograms of the relative humidity with respect to ice measured by the MOZAIC and produced by the ECMWF analysis. Similar to what was found by Nawrath (2002) for the tropical Atlantic, there are three major differences between the MOZAIC and the ECMWF. 1) ECMWF

constantly predicts a drier upper troposphere than the MOZAIC measurements: the mean RH value is 10% - 20% lower for the former than for the latter. 2) The distribution of the MOZAIC UTH is highly bimodal in both deep tropics and subtropics. In contrast, bimodality is hardly seen in the ECMWF analysis. 3) Ice supersaturation is commonly found in the MOZAIC data but becomes virtually nonexistent in the ECMWF. The Asian Monsoon region, for example, sees ice supersaturation 46% of the time during the wet season whereas the ECMWF relative humidity is still cut off sharply at 100%. Some of these differences can be explained by the different resolutions of the two datasets. The temporal/spatial resolutions of the MOZAIC measurements are, respectively, 1 min and 15 km. The ECMWF analysis, on the other hand, represents 6-hourly averages over an area of around 50 km. Zhang et al. (2003) show that averaging can effectively turn the humidity distribution from bimodal to unimodal (which is to be expected from the Central Limit Theorem). This may explain the scarcity of bimodality in the ECMWF analysis and may partially explain the lack of ice supersaturation. However, the virtually total absence of ice supersaturation in the ECMWF indicates that it is probably not allowed in the assimilation system's cloud parameterizations. Finally, the mean dry bias in the ECMWF cannot be explained by the resolution difference since averaging does not change the mean value. Rather, it is mostly likely a real model deficiency which needs to be dealt with seriously.

5. Relation to Transport and Convection

UTH is controlled by the interplay of many processes. Among them, horizontal large-scale transport, subsidence (or uplifting), and deep convection play the dominant role (Luo and Rossow 2004). In this section, we study the horizontal moisture transport (or moisture flux) using the aircraft-measured specific humidity and winds. The connection to deep convection is explored by studying the ISCCP data and the large-scale winds from the NCAR/NCEP reanalysis. Local uplifting and subsidence are hard to measure, but their influences can be inferred from other measurements such as cirrus distribution (Luo and Rossow 2004).

5.1 Aircraft-Measured Moisture Fluxes

Figure 11 shows the composite annual cycle of the horizontal moisture flux at the 239 hPa level. Both specific humidity and wind are measured from onboard the aircraft (see Section 2) and they are composited on a seasonal basis instead of monthly to increase the number of observations. We choose the 239-hPa level because it is a prominent flight level common to all three tropical regions containing most measurements for studying a complete annual cycle. The moisture flux patterns are similar for other levels (not shown) but the magnitude differs from one level to another mainly due to the rapid decrease of water vapor mixing ratio with height.

In general, zonal fluxes are much greater than meridional fluxes because zonal winds are much stronger than meridional winds (Fig. 12). For the tropical Africa, the annual migration of the maximum UTH (Fig. 2) is closely related to the upper-level divergent pattern (Fig. 11) exporting moisture to the corresponding winter hemisphere (i.e., the subsiding branch of the Hadley cell). The meridional wind and meridional moisture flux are especially strong during the boreal summer season, which represents an enhanced meridional circulation. This enhanced circulation may explain the extreme dryness in the Southern Africa during the local dry season (Fig. 5). The moisture flux over the Asian Monsoon region is characterized by the monsoon circulation with reversing wind direction between summer and winter seasons. Tropical Atlantic is somewhat complex: to the south of equator, moisture flux from the Amazon is dominant all year round, while at the equatorial zone, the influence of Amazon and Africa alternate to take control between winter and summer. The influences of these large-scale fluxes and transports will become clearer when analyzing the reanalysis winds from a global perspective in the next subsection.

Fig. 11 shows the total moisture flux, i.e. $\overline{v \cdot q}$. Since we know the seasonal mean velocity (\overline{v}) and specific humidity (\overline{q}), we can calculate the contributions from the mean ($\overline{v \cdot q}$) and the transient ($\overline{v' \cdot q'}$) motions. Figure 13 – 14 show the two contributions based on such a decomposition following Peixoto and Oort (1992). Several interesting findings deserve discussion. First, the mean circulation accounts for the majority of the moisture flux in the tropical upper troposphere; the magnitude of the transient flux is only about 20% of that of the mean motion (note change in scale in Fig. 14). This suggests that the tropical upper tropospheric circulation is, to a large extent, quasi-stationary on the season timescale. Second, transient flux, although generally small, makes a noticeable contribution at some latitudes and seasons. A careful comparison between Fig. 13, 14 and Fig. 2 indicates that the transient contribution usually is a maximum between very moist and very dry regions. For example, the maximum transient meridional flux over tropical Africa (the middle panel on the 2nd row of Fig. 14) is closely sandwiched by the ITCZ and the subtropical dry zone. Newell et al. (1992) proposed a “tropospheric river” concept and used it to describe the observed filamentary structure of the moisture transport. Pierrehumbert (1998) showed that the lateral mixing is an important source of subtropical water vapor and found that the exchange of moisture between tropics and subtropics is achieved through some coherent moist plumes. Our result is consistent with these previous studies showing the importance of the transient moisture

transport in linking the moisture source (deep tropics) and moisture sink (subtropics) regions.

5.2 Transports and Convection from reanalysis and ISCCP

In this subsection, we examine the influence on UTH of the large-scale transport and deep convection in combination. To isolate the strongest and deepest convection, we define convection as that having the satellite-derived cloud-top temperature lower than that of the 180-hPa level, which roughly corresponds to 13 km in the tropics. Convection with its top reaching this height can potentially have a large impact on UTH measured by MOZAIC (which roughly covers the layer from 288 to 197 hPa). Large-scale wind is taken from the NCAR/NCEP reanalysis long-term, monthly mean at the 250-hPa level.

Figures 15 plots simultaneously the seasonal mean deep convection frequency and the 250-hPa wind. The large-scale circulation depicted in the reanalysis is consistent with that measured by the aircraft (Fig. 12). Figs. 15 shows that the regional differences in UTH (Fig. 2) are closely connected to deep convection: the tropical Atlantic has the driest upper troposphere because it hardly has any deep convection of this strength (i.e., strong enough to reach the 180-hPa level); the Asian Monsoon region, on the other hand, has the moistest upper troposphere and the most abundant deep convection during the wet season. Tropical Africa comes in between these two in terms of convective frequency and has a well-paced season migration of convective zone and UTH maximum.

In addition to deep convection, the role of large-scale transport is also shown in Fig. 15. The most notable case is the tropical Atlantic. Since there is rarely any very deep convection (i.e., convection reaching great height) occurring in this region, moisture transport becomes an important agent for affecting the seasonal variation of UTH. Fig. 2 shows that it is relatively moist from the equator to 30S during the boreal winter. Fig. 15 suggests that this seasonal moistening is probably related to the downwind transport of water vapor from convection over the Amazon. We will use a back-trajectory dataset to verify this in our future study. Tropical Atlantic is dry during the boreal summer season because neither local convection nor convective downwind transport makes any significant contribution to UTH.

6. Summary and Conclusion

Ten years of measurements of tropical upper-tropospheric water vapor by the MOZAIC are studied over three selected tropical regions (tropical Atlantic, tropical Africa and the Asian Monsoon region) in the following aspects: 1) characterization of

UTH climatology (including annual cycle, height dependence and distribution) and of UTH interannual and decadal variability; 2) comparison with the ECMWF analysis identifying outstanding bias of the ECMWF product; and 3) examination of the influences on UTH of large-scale transport and deep convection.

The UTH annual cycle keeps pace with the corresponding seasonal migration of the ITCZ highlighting the convective influence on the UTH distribution. Some regional differences are found and they are closely related to the differences in the distribution of deep convection frequency. UTH generally increases with height from 300 to 200 hPa. The instantaneous distribution of tropical UTH is bimodal, as suggested by a number of previous studies. Some intriguing details pertaining to this bimodality are identified in this study. In the deep tropics, the moisture level frequently reaches ice supersaturation and even approaches saturation over liquid. The most notable case is the Asian summer monsoon region where ice supersaturation occurs 46% of the time during the wet season. This is a little surprising considering that aircraft usually flies to avoid major thunderstorms. The two modes in the bimodal UTH distribution stay rather constant at around 20% and 100%; differences in the mean value are largely due to variations in the proportion of the two modes as opposed to changes in modes themselves. This suggests that the two dominant modes are probably a manifestation of two underlying processes that have controlling effects on UTH, presumably convective moistening and subsidence drying. A noticeable interannual variability of UTH is associated with the 1997/1998 ENSO, with the tropical Atlantic becoming drier during the El Niño phase (i.e., winter of 1997-1998) and the Asian Monsoon region getting moister during the following La Niña in the summer of 1998. Tropical Africa seems to be little affected. A surprising moistening trend is found over tropical Africa from 2000 to 2002 (and maybe beyond). The reason for the trend is unknown at the time of writing this paper; further study is needed.

The ECMWF analysis data are interpolated to the MOZAIC measurement coordinates on flights. Comparison between them shows that the ECMWF constantly predicts a drier upper troposphere by 10 – 20 %. Moreover, the bimodality distribution of UTH and ice supersaturation are hardly seen in the ECMWF. Although differences in temporal/spatial resolutions can explain some of these discrepancies, others are related to the deficiencies of the assimilation system. For example, the ECMWF lacks the ability to produce ice supersaturation and underpredicts the mean UTH values.

Meridional and zonal moisture fluxes as measured onboard of the aircraft are studied. Zonal flux is found to dominate the meridional flux. Decomposition of the total flux into contributions from

mean circulation and transient motion shows that the former outweighs the latter by a ratio of 5:1, suggesting that the tropical upper-tropospheric circulation is, to a large extent, quasi-stationary on the seasonal timescale. Transient flux seems to be more significant between very dry and very moist regions serving as an important agent linking the two. Finally, we study the influence on UTH of transport and deep convection from a global perspective using 250-hPa wind from the reanalysis and deep convection frequency from satellite. Many of the UTH climatology features (as found in Section 3 from studying the MOZAIC data alone) are better understood and appreciated from the global view.

References

- Cess and Coauthors, 1990: Intercomparison and interpretation of climate feedback processes in 19 atmospheric general circulation models. *J. Geophys. Res.* **95**, 16601-1665
- Helten, M., H.G.J. Smit, W. Sträter, D.Kley, P. Nedelc, M. Zöger and R. Busen, 1998: Calibration and performance of automatic compact instrumentation for the measurement of relative humidity from passenger aircraft. *J. Geophys. Res.* **103**, 25643-25652.
- Helten, M., H.G.J. Smit, D. Kley, J. Ovarlez, H. Schlager, R. Baumann, U. Schumann, P. Nédélec and A. Marengo, 1999: In-flight intercomparison of MOZAIC and POLINAT water vapor measurements. *J. Geophys. Res.* **104**, 26087-26096.
- Kley, D., J. M. Russell III and C. Phillips (eds), 2000: SPARC assessment of upper tropospheric and stratospheric water vapor, WCRP-No113, WMO/TD - No 1043, SPARC Report No 2. <http://www.aero.jussieu.fr/~sparc/>
- Luo, Z. and W. B. Rossow, 2004: Characterizing tropical cirrus life cycle, evolution, and interaction with upper-tropospheric water vapor using Lagrangian trajectory analysis of satellite observations. *J. Climate*, **17**, 4541-4563
- Mapes, B. E., 2001: Water's two height scales: the moist adiabat and the radiative troposphere. *Q. J. R. Meteorol. Soc.* **127**, 2353-2366
- Marengo, A., V. Thouret, P. Nédélec, H. Smit, M. Helten, D. Kley, F. Karcher, P. Simon, K. Law, J. Pyle, G. Poschmann, R. v. Wrede, C. Hume and T. Cook, 1998: Measurement of ozone and water vapor by Airbus in-service aircraft: The MOZAIC airborne program, an overview. *J. Geophys. Res.* **103**, 25631-25642.
- Mohr, K. I. and E. J. Zipser, 1996: Defining mesoscale convective systems by their 85-GHz ice-scattering signature. *Bull. Amer. Meteor. Soc.*, **77**, 1179-1189
- Nawrath, S., 2002: Water vapor in the tropical upper troposphere: On the influence of deep convection. PhD thesis. Universität Köln. Germany.
- Newell, R. E., N. E. Newell, Y. Zhu and C. Scott, 1992: Tropospheric river? – A pilot study. *Geophys. Res. Letts.*, **12**, 2401-2404
- Peixoto, J. P., and A. H. Oort, 1992: *Physics of Climate*. American Institute of Physics, 520 pp.
- Pieerehumbert, R. T., 1998: Lateral mixing as a source of subtropical water vapor. *Geophys. Res. Letts.*, **25**, 4537-4540
- Pieerehumbert, R. T. and R. Roca, 1998: Evidence for control of Atlantic subtropical humidity by large scale advection. *Geophys. Res. Letts.*, **25**, 4537-4540
- Rossow, W. B. and R. A. Schiffer, 1999: Advances in understanding clouds from ISCCP. *Amer. Meteor. Soc.*, **80**, 2261-2287
- Rossow, W. B., W. Walker, D. Beuschel and M. Roiter, 1996: International satellite cloud climatology project (ISCCP) documentation of new datasets. WMO TECH. DOC. 737, World Climate Research Programme.
- Sherwood, S. C., 1996: Maintenance of free-tropospheric tropical water vapor distribution. Part II: simulation by large-scale advection. *J. Climate*, **9**, 2919-2934
- Waliser, D. E. and C. Gautier, 1993: A satellite-derived climatology of the ITCZ. *J. Climate*, **6**, 2162-2174
- Zhang, C., B. E. Mapes and B. J. Soden, 2003: Bimodality in tropical water vapour. *Q. J. R. Meteorol. Soc.* **129**, 2847-2866

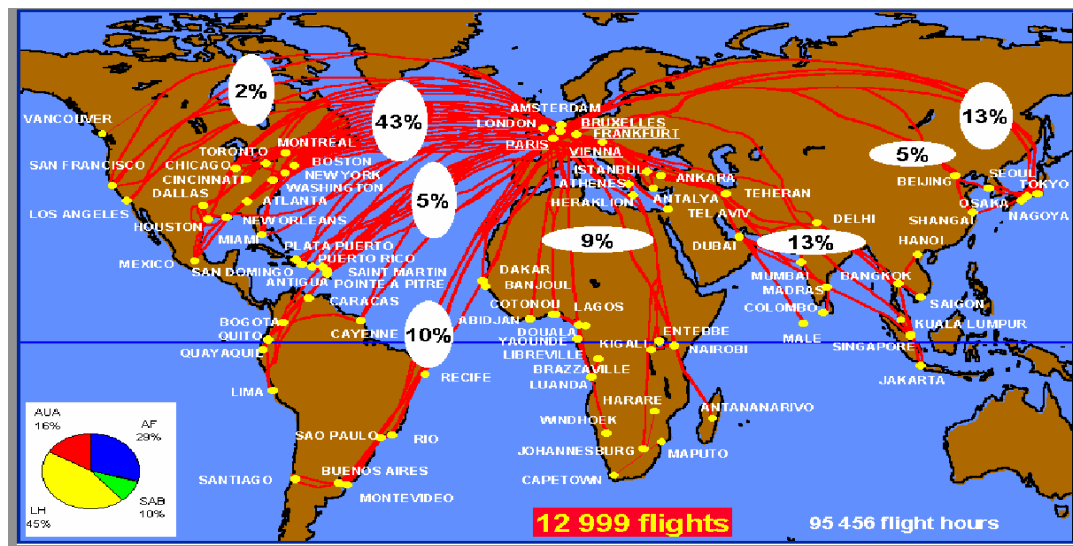


Figure 1. Geographical coverage of the MOZAIC flights from Sept. 1994 to Dec. 1999. The inset depicts the fraction of flights by different airlines.

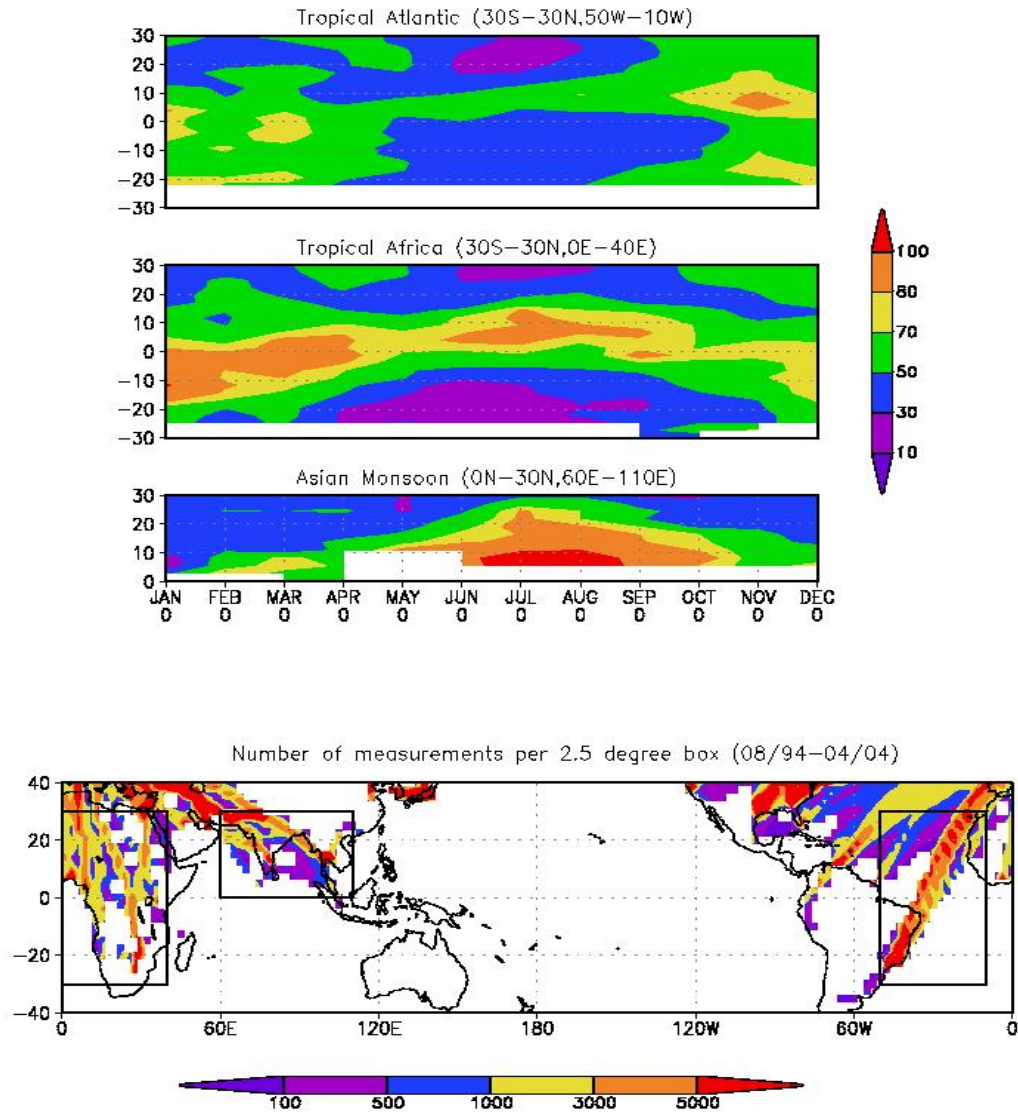


Figure 2. The geographical map of the three tropical regions (lower panel) and the corresponding composite annual cycle of UTH (with respect to ice) as a function of latitude.

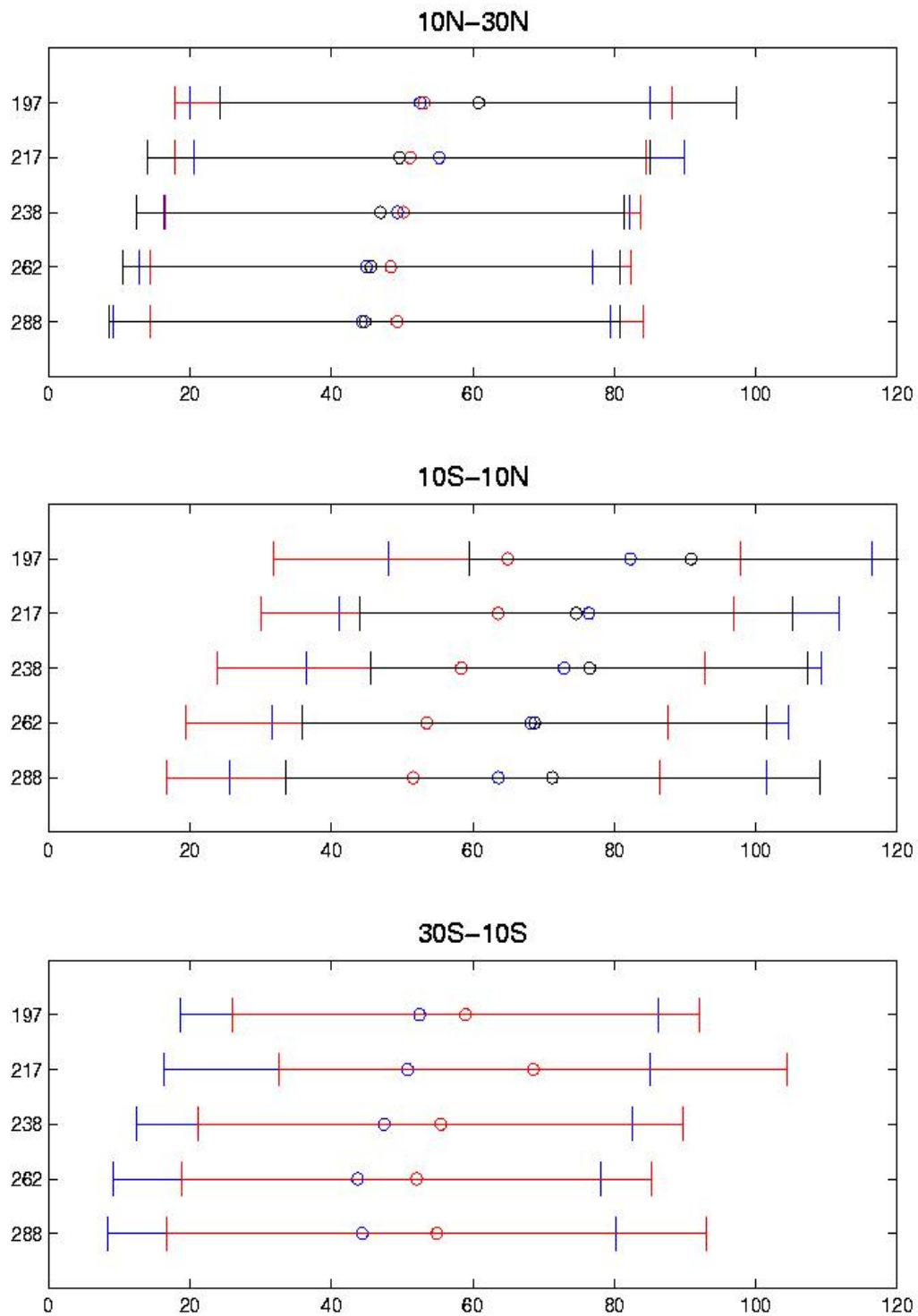


Figure 3. UTH statistics (mean and standard deviation) sorted by pressure level and latitudinal zones. The empty circles and the errorbars are, respectively, the means and the standard deviations. Tropical Atlantic is plotted in red, Tropical Africa in blue, and the Asian Monsoon region in black.

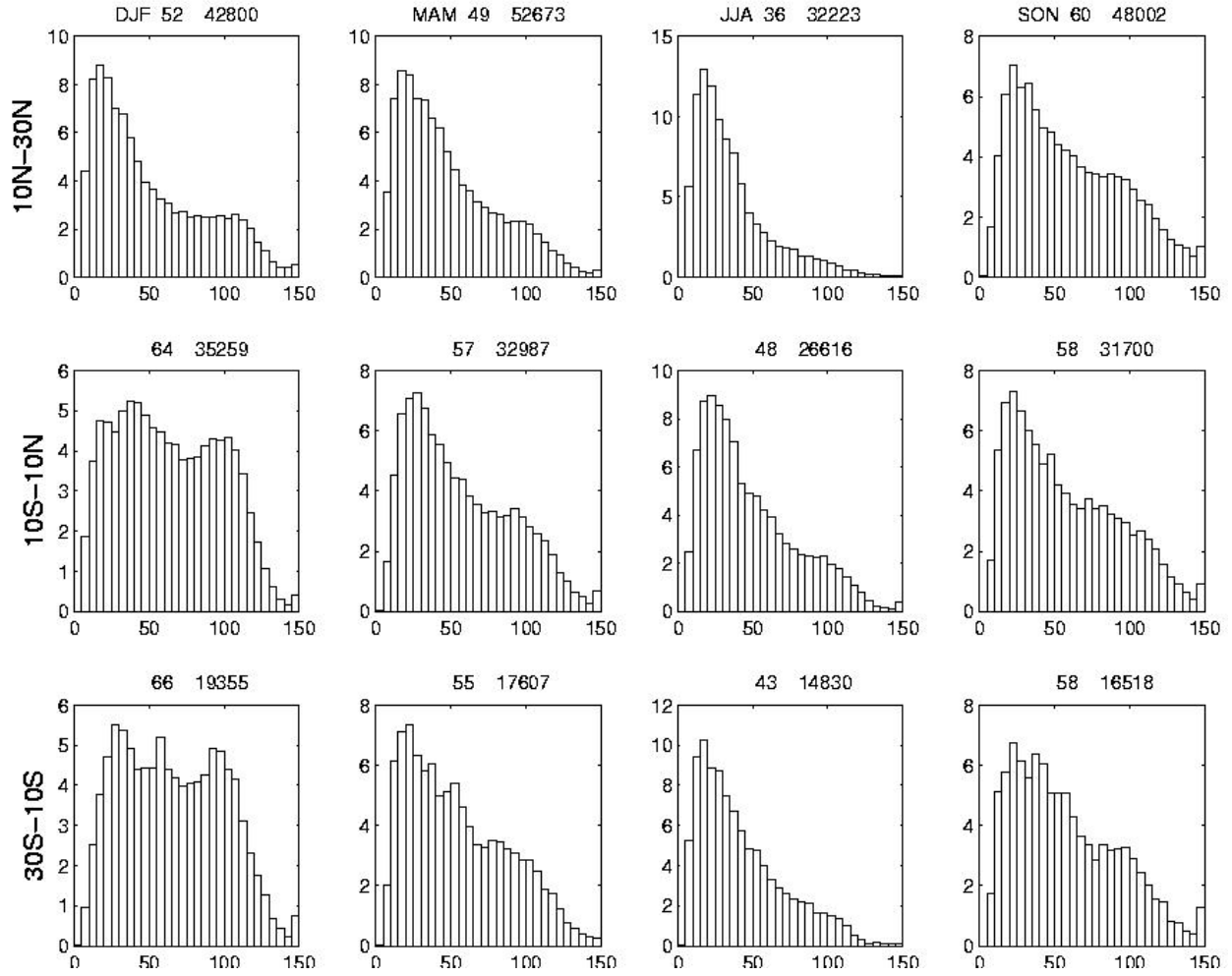


Figure 4. Histograms of UTH for different latitudinal zones and seasons over the tropical Atlantic. The two numbers on top of each panel are, respectively, the mean value and the number of observations.

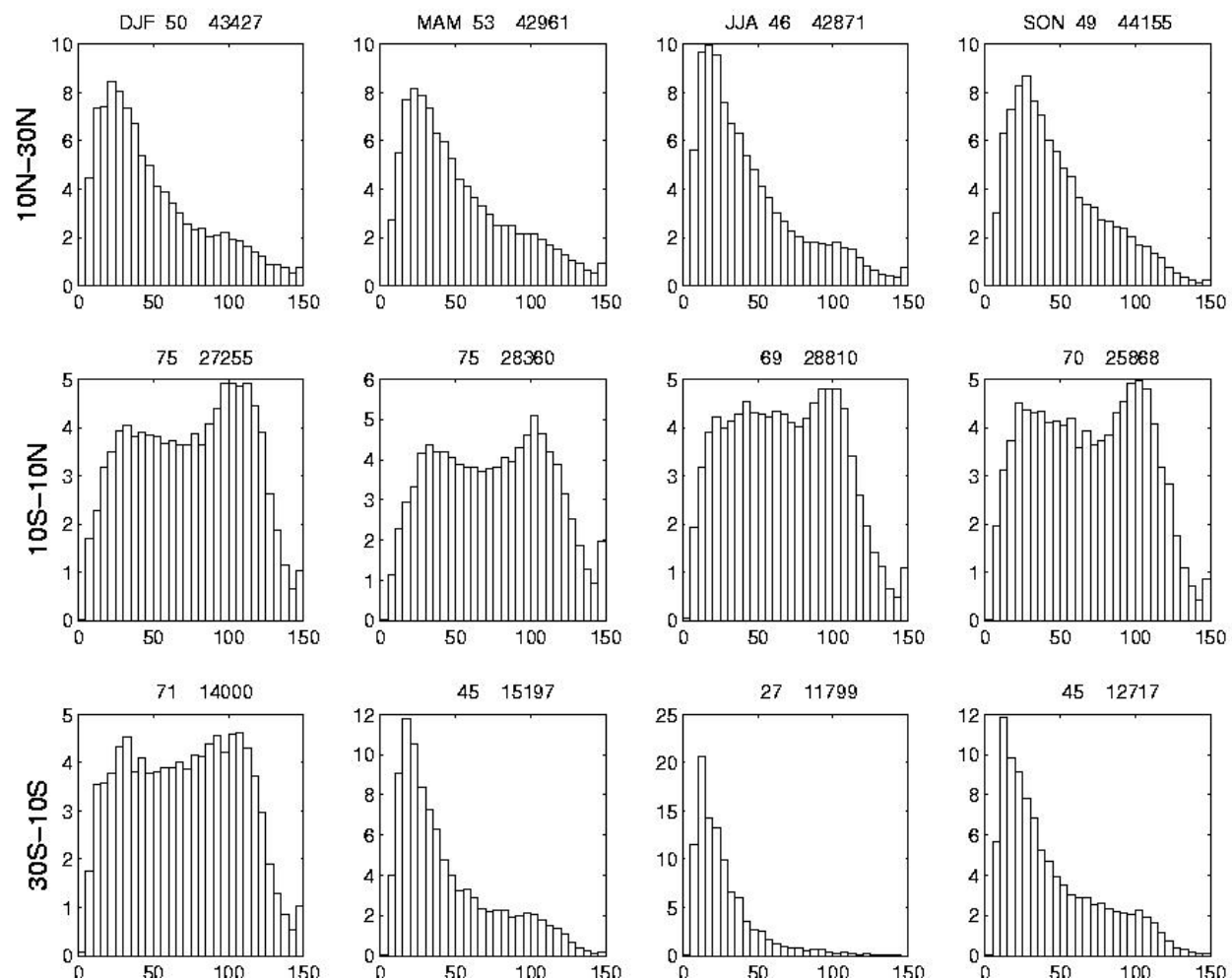


Figure 5. The same as Fig. 4 except for the tropical Africa.

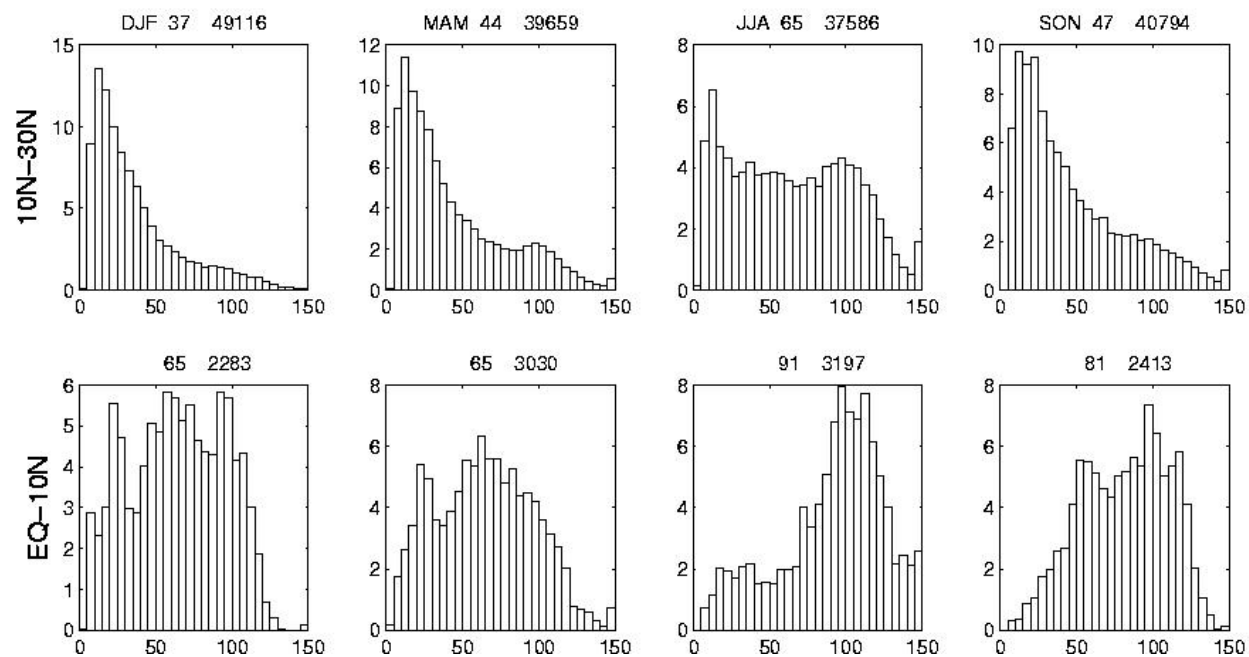


Figure 6. The same as Fig. 4 except for the Asian Monsoon region.

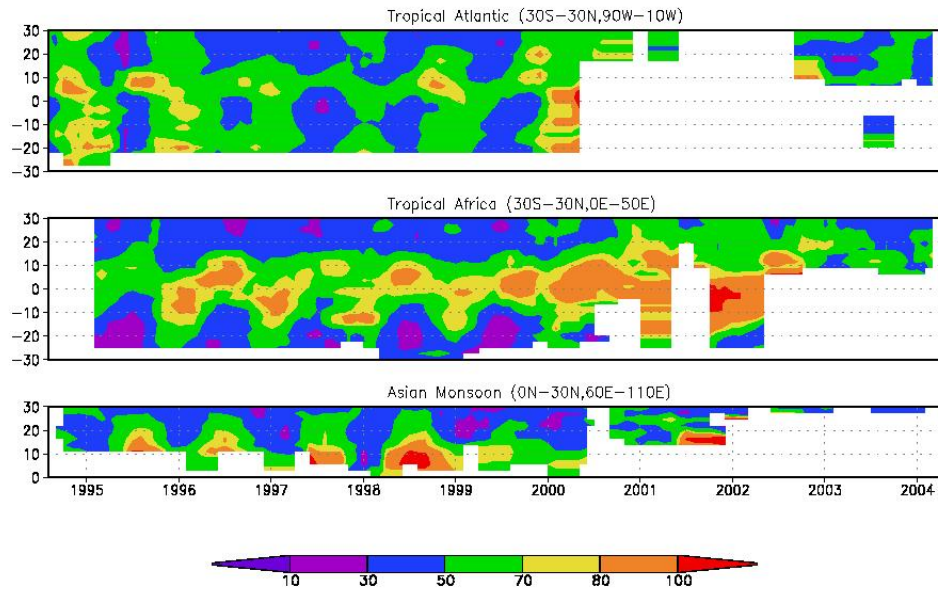


Figure 7. Monthly mean UTH as a function of time and latitude. A 4-month running average window is applied to smooth out some sporadic discontinuity in measurements.

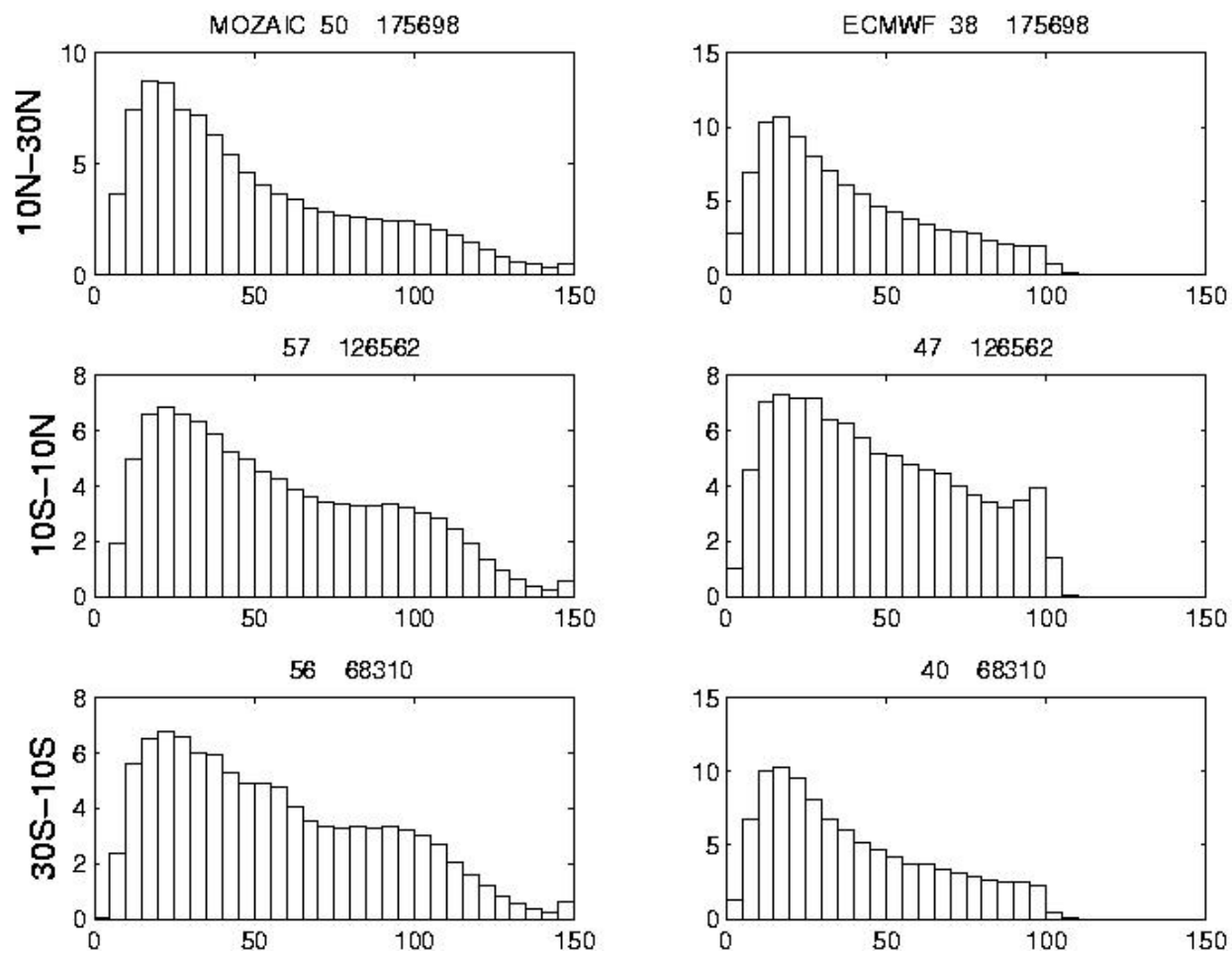


Figure 8. Histograms of UTH measured by the MOZAIC (left columns) and produced by the ECMWF analysis (right column) over the tropical Atlantic. The two numbers on top of each panel are, respectively, the mean value and the number of data.

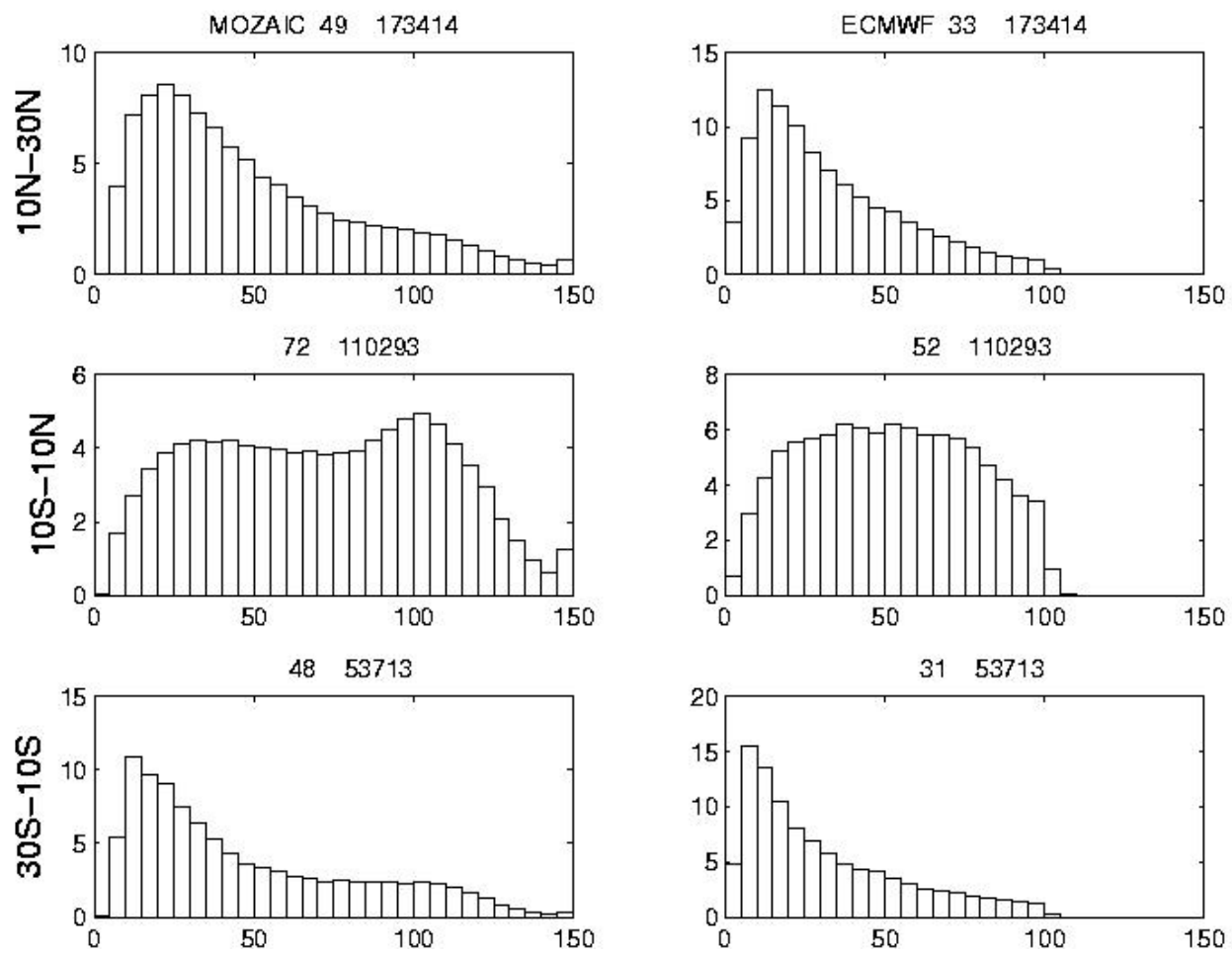


Figure 9. The same as Fig. 8 except for the tropical Africa.

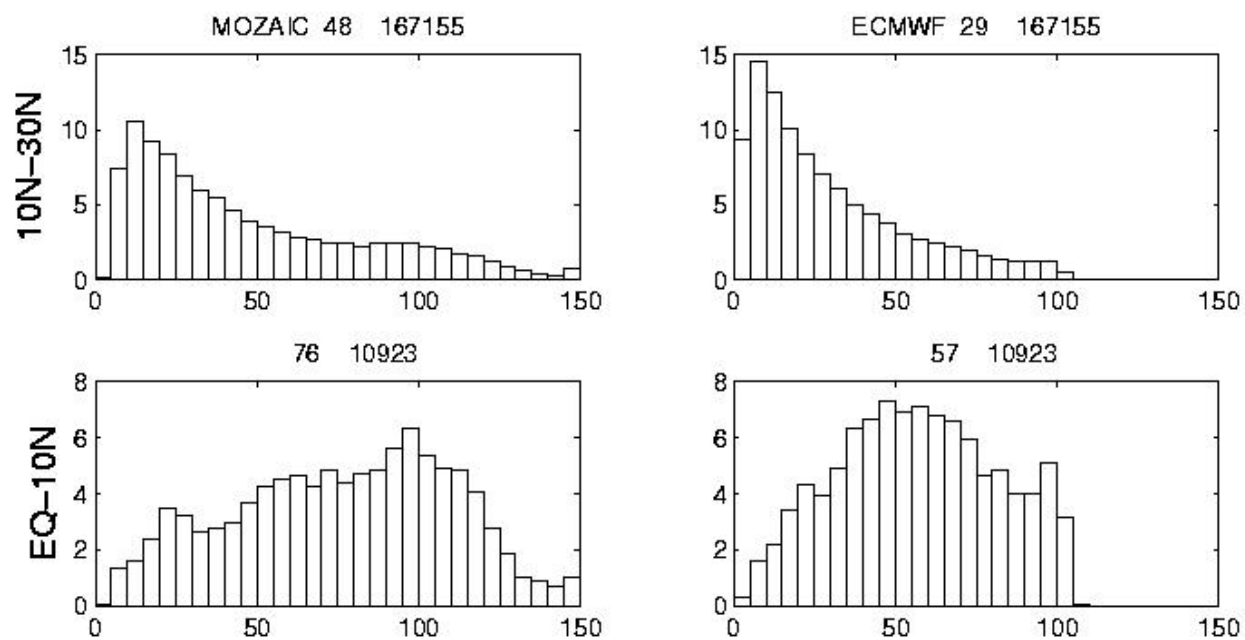


Figure 10. The same as Fig. 8 except for the Asian Monsoon region.

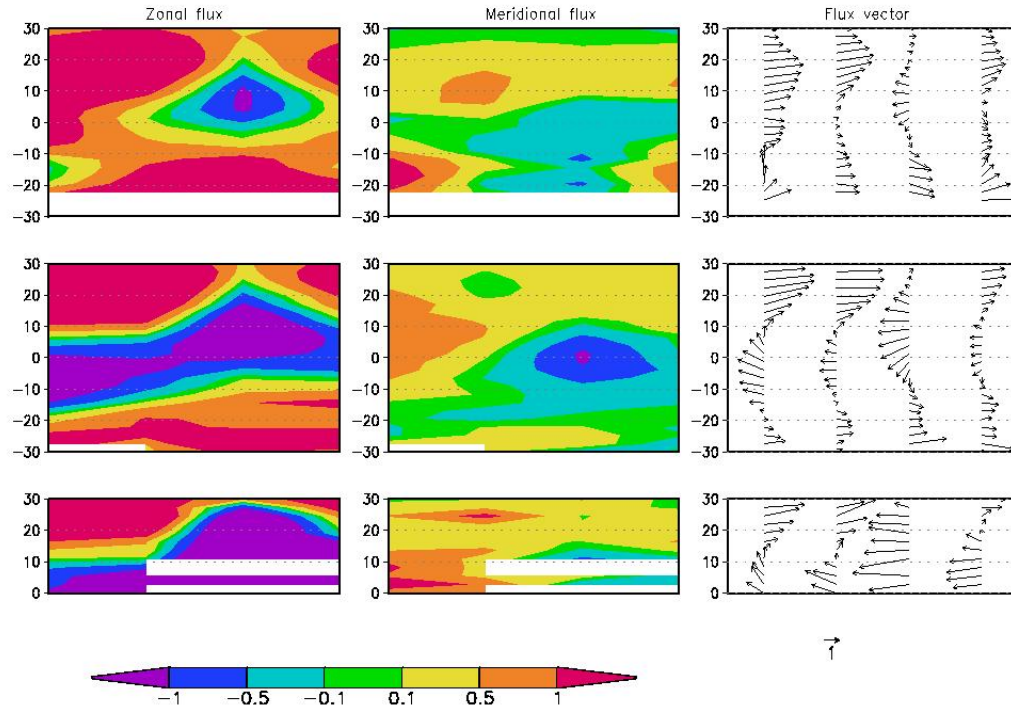


Figure 11. Composite annual cycle of moisture fluxes at the 239 hPa level. The leftmost three panels are for the zonal flux, the middle panels for the meridional flux, and the rightmost panels are the combination of the two in vector forms. The three rows, from top to bottom, correspond to the tropical Atlantic, tropical Africa and Asian Monsoon region, respectively. There are no labels on the x-axes, but they refer to the four seasons of, from left to right, DJF, MAM, JJA, and SON. The units for the contours and the vectors are $(\text{g/kg}) \cdot (\text{m/s})$.

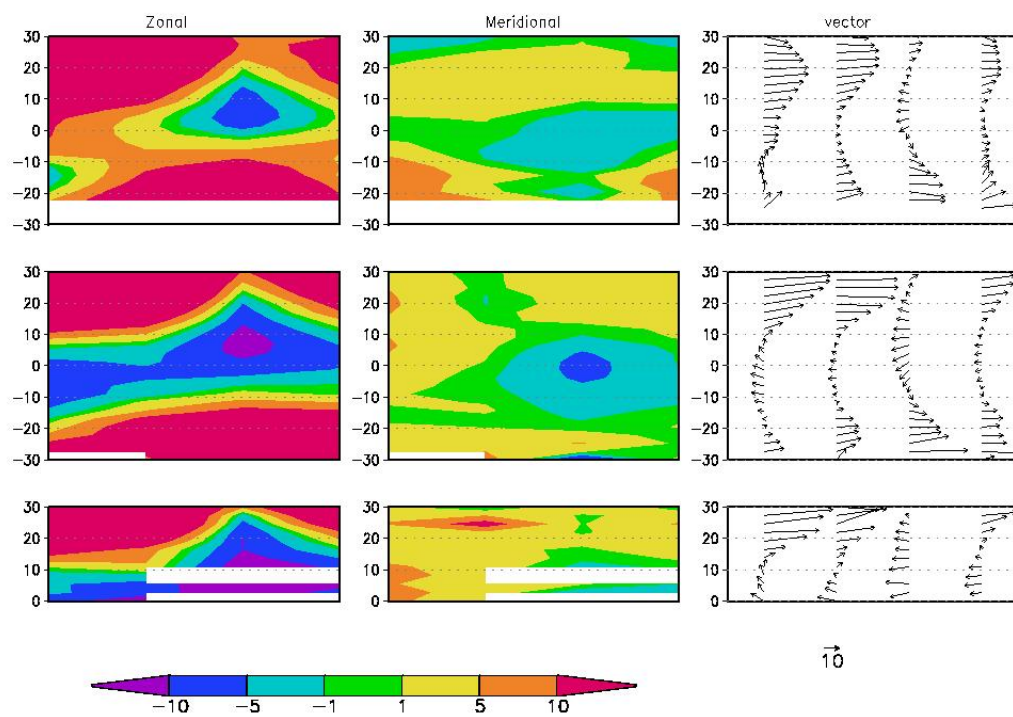


Figure 12. The same as Fig. 11, except for winds. The units are m/s.

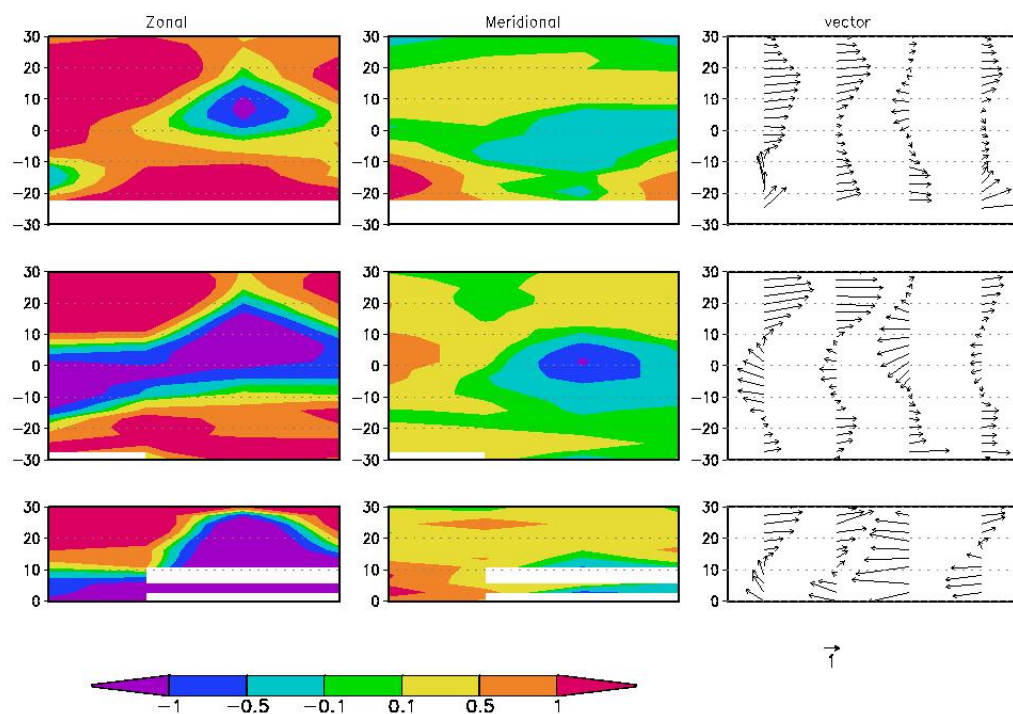


Figure 13. The same as Fig. 11, except for the moisture fluxes by the mean motions. The units for the contours and the vectors are $(\text{g/kg})(\text{m/s})$.

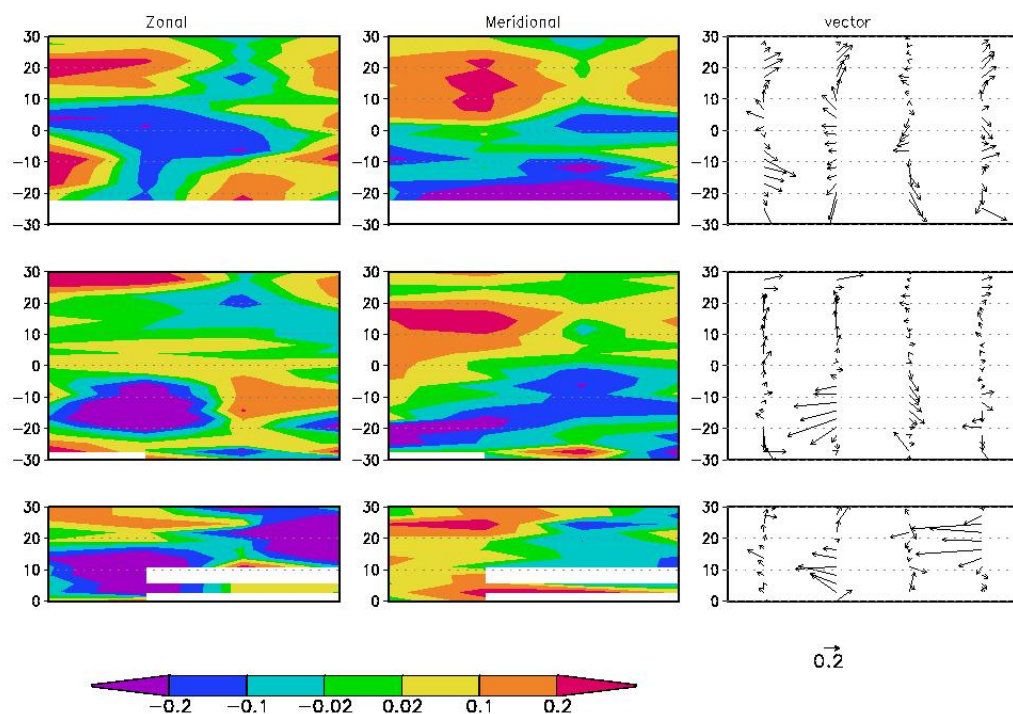


Figure 14. The same as Fig. 11, except for the moisture fluxes by the transient motions. The units for the contours and the vectors are $(\text{g/kg}) \cdot (\text{m/s})$.

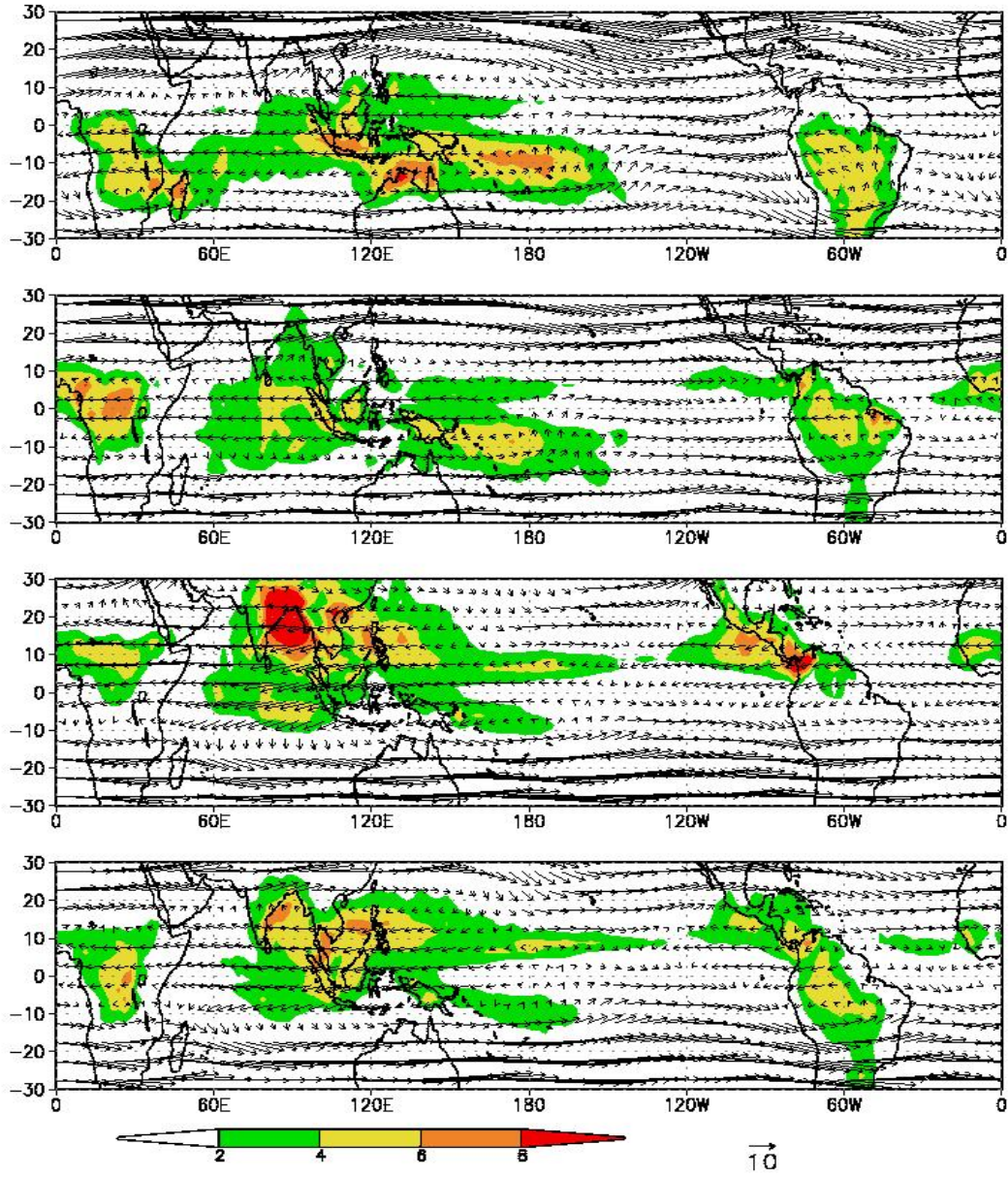


Figure 15. Long-term, seasonal mean deep convection (see text for the definition) frequency from ISCCP (contour) and 250-hPa wind (vector) from the NCAR/NCEP reanalysis. The four panels from top to bottom are, respectively, for DJF, MAM, JJA and SON seasons.